Ferritin Ion Channel Disorder Inhibits Fe(II)/O₂ Reactivity at Distant Sites

Takehiko Tosha,[†,‡] Rabindra K. Behera,[†] and Elizabeth C. Theil*,[†,§]

[†]Children's Hospital Oakland Research Institute, Oakland, California, United States
[§]Department of Nutritional Science and Toxicology, University of California, Berkeley, California, United States

ABSTRACT: Ferritins, a complex, mineralized, protein nanocage family essential for life, provide iron concentrates and oxidant protection. Protein-based ion channels and Fe(II)/O₂ catalysis initiate conversion of thousands of Fe atoms to caged, ferritin Fe₂O₃·H₂O minerals. The ion channels consist of six helical segments, contributed by 3 of 12 or 24 polypeptide subunits, around the 3-fold cage axes. The channel structure guides entering Fe(II) ions toward multiple, catalytic, diiron sites buried inside ferritin protein helices, ∼20 Å away from channel internal exits. The catalytic product, Fe(III)−O(H)−Fe(III), is a mineral precursor; mineral nucleation begins inside the protein cage with mineral growth in the central protein cavity (5−8 nm diameter). Amino acid substitutions that changed ionic or hydrophobic channel interactions R72D, D122R,

and L134P increased ion channel structural disorder (protein crystallographic analyses) and increased Fe(II) exit [chelated Fe(II) after ferric mineral reduction/dissolution]. Since substitutions of some channel carboxylate residues diminished ferritin catalysis with no effect on Fe(II) exit, such as E130A and D127A, we investigated catalysis in ferritins with altered Fe(II) exit, R72D, D122R and L134P. The results indicate that simply changing the ionic properties of the channels, as in the R72D variant, need not change the forward catalytic rate. However, both D122R and L134P, which had dramatic effects on ferritin catalysis, also caused larger effects on channel structure and order, contrasting with R72D. All three amino acid substitutions, however, decreased the stability of the catalytic intermediate, diferric peroxo, even though overall ferritin cage structure is very stable, resisting 80 °C and 6 M urea. The localized structural changes in ferritin subdomains that affect ferritin function over long distances illustrate new properties of the protein cage in natural ferritin function and for applied ferritin uses.
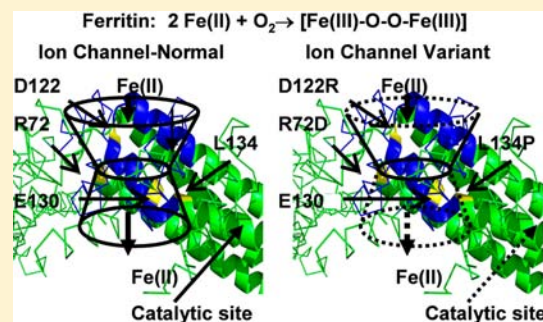
INTRODUCTION

The supramolecular protein family of ferritins synthesizes caged hydrated ferric oxide minerals. Ferritin minerals are metabolic iron concentrates; ferritin protein-based Fe(II)/O₂ catalysis is a physiological antioxidant during biological stress.[1] The ferritin cages, composed of polypeptides that spontaneously fold into bundles of four-α-helices and self-assemble from 12 or 24 subunits, have very high structural symmetry as illustrated in Figure 1. Many studies have shown that the 3-fold symmetry axes in ferritin protein cages are ion channels that control Fe(II) entry for catalysis and Fe(II) exit after mineral dissolution; see recent reviews.[1,2] Ferritin ion channel pores, at the ends of each Fe(II) ion channel, open onto the external (cytoplasmic) or internal surface of ferritin protein cages (Figure 1). At the external pores, the N-terminal sections of each polypeptide subunit extend from the helix bundle and are held in place around the pores by a network of hydrogen and ionic bonds. Disruption of the bonding network increases structural disorder in the N-terminus and increases Fe(II) exit rate, exemplifying molecular "gating".[3]

Another type of ferritin channel was recently identified inside each catalytically active (H or H′ or M) subunit, distal to the active site and distinct from Fe(II) ion channels. This newly discovered set of channels, mineral nucleation channels, was observed by comparing solution NMR of ferritin with and without ferric ions; four aliquots of 48 Fe(II) [8 Fe(II)/diiron nucleation site], added sequentially to ferritin protein cages in air, preceded acquisition of each NMR spectrum.[4] Ferritin nucleation channels in each H-type subunit connect the catalytic sites to the internal mineral growth cavity and are absent in the animal L subunits, which are catalytically inactive. Nucleation channel pores are symmetrically placed around the four—fold symmetry axes of the ferritin cage.[4] Proximity of four nucleation channel exits facilitates protein-based control of ferritin mineral order because mineral nuclei emerging from the nucleation channels spatially oriented by the nucleation channels can readily interact with other mineral nuclei emerging from neighboring, H subunits. Such observations provide a functional explanation for 4-fold symmetry in ferritin protein cages and the relationship between the numbers of protein catalytic sites and nucleation channels with degrees of order in ferritin mineral structures. Thus, the high crystallinity of ferritin minerals from tissues such as heart coincides with a high % of H subunits, and high number of cage catalytic sites and nucleation channels. By contrast, the low mineral order in
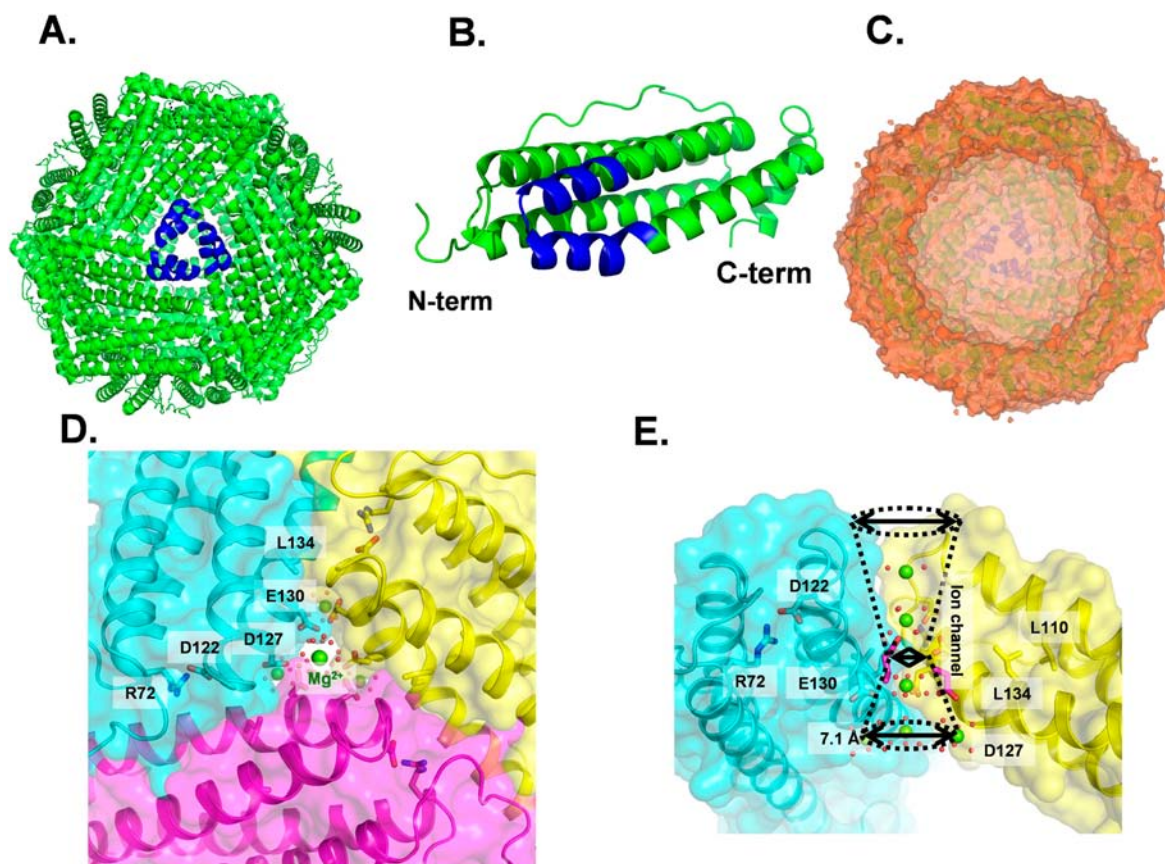
Figure 1. Ferritin (eukaryotic) protein cage structure. Ferritin protein cages with eight Fe(II) entry channels, ~16 Å long, assemble from identical helix segments contributed by three polypeptide subunits, transport Fe(II) from the cage exterior to interior, exiting near the catalytic sites in each subunit. A second type of channel, for ferric oxo nucleation, ~20 Å long, connects catalytic sites to the central mineral growth cavity, moving the Fe(II)/O_2 catalytic product, Fe(III)-O(H)-Fe(III). (A) Ferritin protein cage, outside view with a 3-fold cage axis in the center; blue, helix segments from subunits forming an Fe(II) ion channel. (B) Side view of a polypeptide subunit; blue, helix segments that form an Fe(II) ion channel. (C) Cutaway version of the ferritin protein cage with an empty mineral growth cavity viewed toward a 3-fold axis. Hazy blue helices in the center, an ion channel on the inner cage surface opposite the cut away section. (D) View of a ferritin ion channel from outside the cage. A section of the N-terminal peptide extending from the helix bundle, through a network of bonds to the helices, slows ("gates") the Fe(II) exit during mineral dissolution. Green, Mg(II) ions; red, ordered H_2O. (E) Side view of the 16 Å long, ferritin ion channel; Green - Mg(II) ions. Pore diameters: Outer (top) 8.5; Inner (bottom) 7.1 Å; mid-channel diameter 5.4 Å. Figures from PDB 3KA3 and 3SH6 used PyMol, or Discovery Studio (visualizer), 2.0, for the cage cross section.

ferritin minerals from tissues such as liver coincides with a low % of H subunits, low number of catalytic sites and nucleation channels in each ferritin cage[5] The low order of microbial ferritin minerals, which have a high mineral phosphate content (P/Fe = 1:2) compared to animal ferritin minerals (P/Fe = 1:8), reflects the high phosphate and is protein-independent,[6−10] contrasting with the protein dependence of animal ferritin mineral structure.

Fe(II), one of the two substrates for ferritin oxidoreductase activity, accesses the catalytic sites buried in protein cage through the ion channels around the 3-fold symmetry axes of ferritin protein cages.[10−12] Movement of Fe(II) through the ion channels is regulated, in part, by ion gradients created by the conserved negatively charged residues that line the ion channels.[2,13] However, critical, functional, properties of ferritin ion channel structure depend on stabilization by conserved hydrophobic residues.[3,14,15] In the 12 subunit mini-ferritins (Dps proteins) of bacteria, ion channel carboxylates control both Fe(II) entry and exit but in the more complex ion channels of 24 subunit maxi-ferritins some conserved, ion channel carboxylate residues, such as E130 and D127, selectively control only Fe(II) entry and not Fe(II) exit.[16−18]

Each ferritin ion channel in a 24 subunit protein cage supplies Fe(II) substrate to multiple oxidoreductase sites, since there can be as many as 24 active sites/protein cage (one/subunit) with only 8 ion channels.[1]

As many as three metal ions are observed in clusters near the internal exit of each ion channel in cocrystals of ferritin protein cages with model divalent cations.[12] They appear poised for distribution to three catalytic sites. Active site binding of two Fe(II) at ferritin diiron oxidoreductase sites can be monitored by MCD/CD, in the absence of O_2. A Hill coefficient of three is observed for Fe(II) binding,[19] although Fe(II) binding to each iron binding site in the diiron center is independent; the observation derives from an Fe(II) titration experiment that monitored spectroscopic signals of Fe(II) bound at each of the two sites in ferritin diiron catalytic centers. in the absence of O_2.[19] Because there was no O_2 present and because the binding of two Fe(II) ions to each iron binding site in the diiron center was independent,[19] the positive cooperativity must reflect protein: protein interactions. Such ferritin protein: protein interactions may relate to the distribution of Fe(II) from single Fe(II) ion channels to multiple active sites. Note that confirmation of Fe(II) distribution by Fe(II)-ferritin cocrys-

tallography is difficult because of the very rapid transfer of the Fe(II) substrate to the active site and reaction with the second substrate, O_2 (msec).[1] Computational models based on gradients of negative charge in ferritin ion channels, for example,[13] explain the general behavior of ferritin ion channel residues, but do not explain why different negatively charged channel residues have selective effects.[3] The selective effects of different ion channel carboxylates indicate that properties other than charge influence Fe(II) transport through the ferritin ion channels.[3]

Recent studies[3] of Fe(II) exit during dissolution of the ferritin mineral, using protein cages of ferritin with variant channel residues, revealed a relationship between increased Fe(II) exit and two types of structural effects: (1) Increased flexibility (B′ factor) near the channel entry pores (R72D, D122R) and (2) Increased flexibility throughout the ion channel (D122R) or nearer the diiron catalytic sites (L134P). The change in R72, which is in a helix close to the external pore of each ion channel, caused disruption of the localized network of H and ionic bonds in the helix bundle and the N-terminal peptide that extends outside each helix bundle,[3] (Figure 1B, Table 1).

Table 1. Sites of Structural Disorder in Variant Ferritins[a]

proteins	disordered residues compared to wild type	helices affected
R72D	1−15	Helix 1
D122R	5 −15, 100−140	Helix 1, Helix 3, Helix 4
L134P	123−135	Helix 3

[a]B′-factors values are 2−4 times greater than wild type, as determined from XRD of protein crystals, 1.5 Å resolution.[3] The N-terminal extension includes residues 1−11 and the channel residues are 110−134; helix 3 has residues 92−119 and helix 4 has residues 125−155.

In R72D, the structural changes and the functional changes in Fe(II) exit identified the gating function of the N-terminal peptide[3] at the external (cytoplasmic) pores of ferritin ion channels. In L134P ferritin cages, the substitution of a conserved amino acid in the channel that forms stabilizing helix−helix interactions with ion channel residue (L110),

caused structural disorder in the channel itself (Table 1) and increased Fe(II) exit rates, thereby revealing the role of the ion channels in dissolution of caged ferritin minerals and caged Fe(II) exit.[14] Here we examine the effects of the structural changes in R72D, D122R and L134P on Fe(II) entry and ferritin oxidoreductase activity, by monitoring the formation and decay rates of the diferric peroxo (DFP, Fe(III)−O−O− Fe(III)−DFP) catalytic intermediate.

■ EXPERIMENTAL SECTION

The Fe(II) ion entry/exit channel mutants (R72D, D122R, and L134P) in M-ferritin protein cages were generated by QuikChange Mutagenesis (Stratagene),[3] using the extensively characterized frog (R. catesbeiana) M ferritin model; recombinant proteins were purified from E. coli as previously described.[15,20] The final buffer for the proteins was 100 mM MOPS (pH 7.0) and 100 mM NaCl. Protein concentrations were determined by the Bradford method (Biorad protein assay kit) with bovine serum albumin as a standard. Residual iron, determined as the Fe(II)−1,10-phenanthroline complex, was <0.05 Fe/ferritin protein subunit (1.2 Fe/cage).

Ferritin solutions, 0.1 mM subunit (0.0042 mM protein cage), in 200 mM MOPS·Na, pH 7.0, 200 mM NaCl, were mixed with an equal volume of fleshly prepared $FeSO_4$ solution (0.2 mM in 1.0 mM HCl) in a stopped-flow, UV/vis spectrophotometer (Applied Physics). Data were collected at $Abs_{650 nm}$, the absorbance maximum of DFP intermediates in ferritin, and $Abs_{350 nm}$, the nonspecific absorbance of Fe(III)−O species that includes DFP, ferric oxo/hydroxo dimers, multimers and the protein-caged, ferric oxide mineral. Data were collected from 2 to 3 independent preparations of each protein measured 2−3 times each. Initial rates (V_i) were obtained from linear fitting to the early time domain (∼ 50 ms) of $Abs_{350 nm}$ and $Abs_{650 nm}$ data. DFP decay rates were calculated by single exponential fitting to the decay process of the traces at $Abs_{650 nm}$. Data analysis was performed with Igor software (WaveMetrics). The statistical significance of differences was determined using the student t test.

■ RESULTS

The three-ferritin ion channel amino acids that were modified,[21] R72, D122, and L134, are conserved in all eukaryotic ferritins and in some microbial ferritins. In general, ion channel sequences are highly conserved: 84% (conservative substitution) and 52% (absolute) among vertebrates. Multiple ferritin genes code for natural amino acid substitutions that
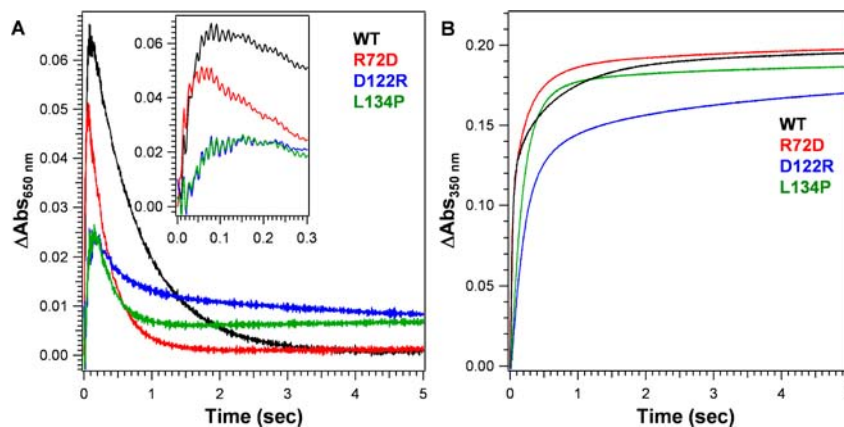
Figure 2. Progress curves of diferric peroxo formation in ferritin M. Fe(II) was added to solutions of frog M ferritin (wild type or with amino acid substitutions at pore residues) in air 25 °C. The ratio of Fe(II): diiron oxidoreductase site = 2 (Total Fe = 48/cage). The absorbance was monitored at 650 nm during ferritin catalysis, which is the λ_{max} for ferritin Fe(III)−O−O−Fe(III) (DFP). DFP forms in msec and decays ∼1 s. at A350 nm is most informative for later stages of mineralization; some studies monitor the absorbance at 310 nm instead, since the transition is broad. Absorbance in the 300−400 nm range is due to a mixture of spectroscopically unresolved species that includes ferric oxo/hydroxo dimers, other multimers and caged $Fe(III)(OH)_6$ mineral. (A) Progress curve for DFP (inset shows data from the early time domain); (B) Ferric oxo/hydroxo formation.

Table 2. Ferroxidase Kinetics: DFP (Diferric Peroxo) Formation and Decay in Wild Type and Variant Eukaryotic Ferritins

sample	DFP formation rate ($V_i{}^a$)		DFP decay rate constant	
	($\Delta Abs_{650\ nm}$/sec)	normalized	(sec^{-1})	normalized
WT	1.50 ± 0.20	1.00	1.48 ± 0.11	1.00
R72D	1.60 ± 0.30	$\mathbf{1.07 \pm 0.25}$	3.15 ± 0.25^b	2.12 ± 0.17^b
D122R	$0.36 \pm 0.03^{b,c}$	$\mathbf{0.24 \pm 0.02}^{b,c}$	2.77 ± 0.23^b	1.87 ± 0.15^b
L134P	$0.31 \pm 0.03^{b,c}$	$0.21 \pm 0.02^{b,c}$	3.64 ± 0.20^b	2.46 ± 0.14^b

[a]Initial rates were obtained from linear fitting to the early time domain (~ 50 ms) of Δ Absorbance at 650 nm. [b]Significantly different than wild type, $P < 0.01$. [c]Significantly different than R72D, $P < 0.01$.

create ferritin protein cages with different combinations of subunit amino acid sequences specific to each tissue, such as animal liver and heart or plant leaf and stem. By contrast, the amino acids studied here, R72, D122 and L134 are encoded in all ferritin genes. Among the variations in multiple ferritin genes is a set of residues, which confer higher or lower ion channel stabilization from interhelical hydrophobic interactions. In such cases the functional and structural effects of the same amino acid substitution, L134P, appear to reflect the amino acid side chain variations and the associated difference in ion channel structure.[3,12] The single amino acids substitutions studied here increased flexibility for multiple channel amino acids (Table 1) which indicates structural integration within the ion channels of ferritin proteins cages.[3]

The initial rate for DFP formation in R72D ferritin was indistinguishable from the wild type (Figure 2, Table 2), contrasting with the significant increase in Fe(II) exit rate.[3] Metal ion binding in the channels of R72D, observed in protein−Mg(II) cocrystals, had few changes.[3]

However, one of the metal ions is bound through water to D72, rather than nearby T118 as in wild type ferritin; another site in wild type ferritin, S131, E130, D127, is also missing in R72D.[3] The significant increase in the oxidation of Fe(II) in R72D, monitored as the absorbance increase at 350 nm (Table 3), which does not occur with DFP formation, could reflect the

Table 3. Kinetics of formation of Fe(III)-O^a formation in variant ferritins

sample	Fe(III)−O^a formation rate ($V_i{}^b$)	
	($\Delta Abs_{350\ nm}$/sec)	normalized
WT	0.82 ± 0.09	1.0
R72D	1.03 ± 0.05^b	$1.25 \pm 0.06^{c,d}$
D122R	$0.27 \pm 0.05^{b,c}$	$0.39 \pm 0.07^{c,d}$
L134P	$0.15 \pm 0.06^{b,c}$	$0.18 \pm 0.08^{c,d}$

[a]The species containing Fe(III)-O unit which includes DFP, ferric oxo/hydroxo dimers, multimers and the protein-caged ferric oxide mineral. [b]Initial rates were obtained from linear fitting, first ~ 50 ms, of $\Delta Abs_{350\ nm}$. [c]Significantly different than wild type, $P < 0.003$. [d]Significantly different than R72D, $P < 0.003$.

impact of the faster decay of DFP on the formation of other ferric oxo/hydroxo species. The accelerated DFP decay in R72D ferritin indicates that the effects of localized structural changes in the ion channels influenced active sites ~ 25 Å away, even though, overall, the protein cage itself is unusually stable.

Depending on the particular change in ferritin ion channel structure, the rate of absorbance changes at $A_{350\ nm}$ (ferric oxo species) increased or decreased, depending on the amino acid substitution. DFP formation, $A650_{nm}$, by contrast, was either unaffected (R72D) or decreased (D122R, K134P) (Table 3). The increase in the rate of change at $A350_{nm}$ may reflect the

impact of faster decay of the diferric peroxo intermediate in R72D on the multiple ferric oxo species present.

The broad absorbance band, measured in this study at 350 nm, includes contributions of DFP, diferric oxo, ferric- oxo multimers (mineral nuclei), mineral itself and possibly some new species in altered ferritins such as R72D. Resolution of the many components absorbing in the range 300−400 nm has not been achieved in contrast to the specific UV−vis properties of the diferric peroxo intermediate with a $\lambda_{max} = 650$ nm. The accelerated DFP decay in R72D ferritin (Table 2) indicates that the even within the rigid protein "shell" of the ferritin cage (stable to 6 M urea and 80 °C), there is sufficient conformational flexibility for structural changes in the ion channels to influence function over long distances (~ 25 Å).

In L134P and D122R ferritin, formation of DFP was significantly inhibited (Figure 2, Table 2) $\sim 80\%$ for both ferric oxo/hydroxo species, contrasting with R72D; DFP stability also changed in L134P and D122R, decreasing by $\sim 60\%$. The decrease in DFP stability (Table 2), emphasizes that changes in ion channel structure and Fe(II) transit within ferritin ion channels can influence intracage reactions spatially separated from the ion channels. The increased flexibility of L134P ferritin ion channels is localized and near the ion channel exits inside ferritin cages. Metal ion binding exhibited decreased occupancy at most ion channel sites with elimination of any metal binding at the three D127 residues where a cluster of metal ions occurs in wild type protein.[3,22] The D122R substitution caused the most structural and functional disorder in ferritin Fe(II) ion channels of the three variant ferritin proteins studied (Table 1).[3] Only one metal ion was observed in Fe(II) ion channels of D122R-Mg(II) cocrystals (Figure 3). In D122R the single metal ion bound in each Fe(II) ion channel is in a constriction formed by the cluster of three E130 residues, one from each of the subunits that form the ion channels. Similarities in the Fe(II)/O₂ reactions at the oxidoreductase sites in D122R and L134P ferritins (Table 2) contrast with the larger effects of D122R on Fe(II) exit during mineral dissolution,[3] and emphasize the differential effects of ferritin ion channel residues and structure on Fe(II) exit during mineral dissolution and entry/active site access.

■ DISCUSSION

Ferritin protein cages are water and saline soluble macromolecular polypeptide assemblies that facilitate Fe(II) transport through protein ion channels. Protein assemblies that facilitate transport K(I), Ca(II), and Na(I), such as those in membranes of living cells, by contrast with ferritin, are much less accessible for study in the native environment. For ferritin ion channels, moreover, the effective transport of Fe(II) through the ion channels, can be specifically measured as the Fe(III)−O−O−Fe(III) catalytic intermediate, contrasting with membrane ion
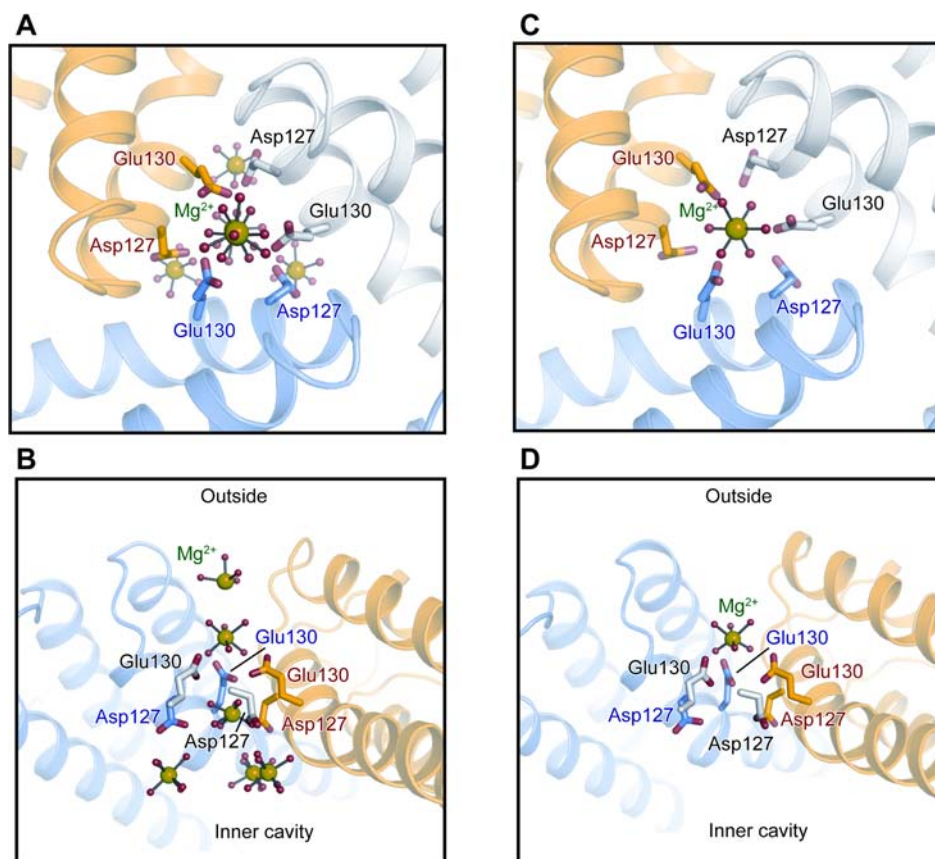
Figure 3. Effect of changes in ferritin ion channel structure on metal ion binding. Figures were drawn with PyMol software, using PDB files WT-3KA3 (A,B); (C,D) D122R-3SH6. (A) WT Fe(II) channel viewed from the top; (B) WT Fe(II) channel viewed form the side. (C) D122R channel viewed from the top; (D) D122R viewed from the side. Green: Mg(II); red: H₂O.

channels where the molecular destination of the ion after channel transport is often undefined. Fe(II) ion channels in ferritin protein cages are analyzed in crystal structures using "surrogate" ions that are not substrates, since Fe(II) moves through the ion channels and reached the active sites within msec; such surrogate metal ions include Mg(II) and Co(II) cocrystals or Cu(II) soaking;[3,22] 6−7 ions can be observed in the channels mainly at carboxylate residues. After soaking ferritn protein crystals in solutions of Fe(III) in air, only 1 Fe(III) atom was bound in the channel, at the three E130 carboxylates in the ion channel constrictions; the other Fe(III)) atoms were bound were at or near active site carboxylate residues. The results with Co(II) are similar to Fe, but different from Cu(II), indicting the metal selectivity of ferritin ion channel environments.[3,22] Fe(II) itself has not yet been trapped in the ion channels of eukaryotic ferritin protein crystals.

Here, by exploiting the ability to monitor Fe(II) flow through the ion channels of the ferritin protein cage and the cage itself, as the kinetics diferric peroxo formation (msec) and decay (sec) we see that: (1) Changes in ferritin ion channel structure, whether by changing hydrophobic or charged amino acids, can slow but not prevent Fe(II) or O₂ access to the active sites (DFP formation), illustrating the dominance of channel structure over localized carboxylate binding; (2) Changes in ferritin channel structure, even though long distances away from the channel exits, influence catalysis since DFP stability declines in all three variants studied, R72D, D122R and L134P. Whether it is Fe(II) or O₂ access to the active sites or Fe/O₂ reactivity that is inhibited by structural changes in ferritin ion

channels is not known. In the ion gradient model for Fe(II) transit, the simple increase in carboxylate electronegativity through the channels to the active sites depends on specific folding of the polypeptide to achieve the needed charge distribution. The influence of complex protein: protein interactions on Fe(II) reactivity in ferritin protein cages is further illustrated by a Hill coefficient of 3 for the directly observed (MCD/CD), and independent binding of Fe(II) at each position in the diiron catalytic sites in the absence of O₂ (MCD/CD);[19] changes in ferritin function [decreased Fe(II) oxidation and Fe(III)₂O₃·H₂O mineral reduction/dissolution] also occur when ferritin protein subunits are fixed in position with chemical cross-links.[4,23] Thus, the new data here complement the earlier data to show the influence of complex, flexible, protein:protein interactions within the unusually stable protein cage on the transport and reactions of Fe(II) in ferritin.

The impact of ferritin ion channel structure itself, distinct from specific Fe(II) ionic interactions with channel carboxylates, on catalysis at the middle of each ferritin cage subunit illustrates the contributions of the 3-fold symmetry axes to ferritin function: structural changes in and around the 3-fold axes not only affected rates at which Fe(II) iron arrived at the active sites (DFP formation), they altered rates of Fe(III) departing the active sites. Earlier studies showed that changes in ferritin nucleation channels around the 4-fold symmetry axes of ferritin cages also influenced Fe(III) leaving the active sites.[4,16−18] Thus, both the residues near the N-termini of ferritin subunits at the 3-fold symmetry axes and those near the C-terminal at the 4-fold symmetry axes alter rates at the active

sites in the middle of each subunit, which in turn affect mineral growth and order.[1] Such observations suggest a connection between the 3- and 4-fold structural symmetry of assembled ferritin nanocages and function. Ferritin protein cage symmetry persists even though ferritin amino acid sequences diverge up to 80%. Further suggesting that the structural subdomains of ferritin cages are preserved by natural selection and thus are related to function. As awareness of the relationships between the structural and functional properties of ferritin protein cages expand, including functional integration of cage subdomains, ferritin nanocage symmetry can be exploited in the synthesis of new, organized, nanomaterials.

■ AUTHOR INFORMATION

Corresponding Author

*Tel: 510-450-7670. Fax: 510-597-7131. E-mail: etheil@chori.org.

Present Address

‡Biometal Science Laboratory, RIKEN SPring-8 Center, Kouto, Sayo, Hyogo 679−5148, Japan

Notes

The authors declare no competing financial interest.

■ ACKNOWLEDGMENTS

■ REFERENCES

(1) Theil, E. C. *Curr. Opin. Chem. Biol.* **2011**, *15*, 304.

(2) Chiancone, E.; Ceci, P. *Biochim. Biophys. Acta* **2010**, *1800*, 798.

(3) Tosha, T.; Behera, R. K.; Ng, H.-L.; Bhattasali, O.; Alber, T.; Theil, E. C. *J. Biol. Chem.* **2012**, *287*, 13016.

(4) Turano, P.; Lalli, D.; Felli, I. C.; Theil, E. C.; Bertini, I. *Proc. Natl. Acad. Sci. U.S.A.* **2010**, *107*, 545.

(5) Pierre, T., St; Tran, K. C.; Webb, J; Macey, D. J.; Heywood, B. R.; Sparks, N. H.; Wade, V. J.; Mann, S; Pootrakul, P *Biol. Met.* **1991**, *4*, 162.

(6) Mann, S.; Williams, J. M.; Treffrey, A.; Harrison, P. M. *J. Mol. Biol.* **1987**, *198*, 405.

(7) Rohrer, J. S.; Islam, Q. T.; Watt, G. D.; Sayers, D. E.; Theil, E. C. *Biochemistry* **1990**, *29*, 259.

(8) Waldo, G. S.; Wright, E.; Wang, Z. H.; Briat, J. F.; Theil, E. C.; Sayers, D. E. *Plant Physiol.* **1995**, *109*, 797.

(9) Wade, V. J.; Treffry, A.; Laulhere, J.-P.; Bauminger, E. R.; Cleton, M. I.; Mann, S.; Briat, J.-F.; Harrison, P. M. *Biochim. Biophys. Acta* **1993**, *1161*, 91.

(10) Le Brun, N. E.; Crow, A.; Murphy, M. E.; Mauk, A. G.; Moore, G. R. *Biochim. Biophys. Acta* **2010**, *1800*, 732.

(11) Chiancone, E.; Ceci, P.; Ilari, A.; Ribacchi, F.; Stefanini, S. *Biometals* **2004**, *17*, 197.

(12) Tosha, T.; Ng, H. L.; Bhattasali, O.; Alber, T.; Theil, E. C. *J. Am. Chem. Soc.* **2010**, *132*, 14562.

(13) Takahashi, T.; Kuyucak, S. *Biophys. J.* **2003**, *84*, 2256.

(14) Takagi, H.; Shi, D.; Ha, Y.; Allewell, N. M.; Theil, E. C. *J. Biol. Chem.* **1998**, *273*, 18685.

(15) Liu, X.; Jin, W.; Theil, E. C. *Proc. Natl. Acad. Sci. U.S.A.* **2003**, *100*, 3653.

(16) Levi, S.; Luzzago, A.; Franceschinelli, F.; Santambrogio, P.; Cesareni, G.; Arosio, P. *Biochem. J.* **1989**, *264*, 381.

(17) Treffry, A.; Bauminger, E. R.; Hechel, D.; Hodson, N. W.; Nowik, I.; Yewdall, S. J.; Harrison, P. M. *Biochem. J.* **1993**, *296*, 721.

(18) Haldar, S.; Bevers, L. E.; Tosha, T.; Theil, E. C. *J. Biol. Chem.* **2011**, *286*, 25620.

(19) Schwartz, J. K.; Liu, X. S.; Tosha, T.; Theil, E. C.; Solomon, E. I. *J. Am. Chem. Soc.* **2008**, *130*, 9441.

(20) Tosha, T.; Hasan, M. R.; Theil, E. C. *Proc. Natl. Acad. Sci. U.S.A.* **2008**, *105*, 18182.

(21) Jin, W.; Takagi, H.; Pancorbo, N. M.; Theil, E. C. *Biochemistry* **2001**, *40*, 7525.

(22) Bertini, I.; Lalli, D.; Mangani, S.; Pozzi, C.; Rosa, C.; Theil, E. C.; Turano, P. *J. Am. Chem. Soc.* **2012**, *134*, 6169.

(23) Mertz, J. R.; Theil, E. C. *J. Biol. Chem.* **1983**, *258*, 11719.